Exame de Proficiência em Língua Inglesa – Nível Doutorado

Instruções: Leia atentamente o texto abaixo e responda às questões propostas. Para as respostas, a Língua Portuguesa deve ser empregada para maioria das Questões. Digite as respostas no espaço apropriado. Não escreva seu nome na Prova ou use qualquer tipo de identificação.

ELSEVIER

Contents lists available at ScienceDirect

Advances in Industrial and Manufacturing Engineering

journal homepage: www.journals.elsevier.com/advances-in-industrial-and-manufacturing-engineering

Analysis of material positioning towards microstructure of the friction stir processed AA1050/AA6082 dissimilar joint

Velaphi Msomi *, Sipokazi Mabuwa

Cape Peninsula University of Technology, Mechanical Engineering Department, P.O. Box 1906, Bellville, 7535, South Africa

ARTICLEINFO

Keywords:
Friction stir welding
Friction stir processing
Microhardness
Microstructure
Tensile tests

ABSTRACT

Friction stir processing (FSP) is considered to be the newly developed technique which was derived from the welding technique called friction stir welding (FSW). This technique modifies the microstructure of the material through stirring. The initial focus of this technique was on processing single surface. The focus has now been extended to the joints. This paper reports on the influence of material positioning during the friction stir processing of the friction stir welded AA1050/AA6082 dissimilar joint. The grain size for the stir zone was found to be finer when AA6082 was positioned on the advancing side during both friction stir welding and processing (with different grain size range). The ultimate tensile strength (UTS) and yield strength (YS) were found to be higher when AA6082 was positioned on the advancing side than when AA1050 on the advancing side during FSW and FSP. It was further observed that the percentage elongation doubled that of the base materials for both FSW and FSP dissimilar joint when AA1050 was positioned on the advancing side.

1. Introduction

Friction stir welding (FSW) is a state-of-the-art solid-state joining process that was developed and patented by The Welding Institute, in 1991 (Dawes and Thomas, 1996). FSW functioning depends on a non-consumable tool that performs the task of stirring the plasticized material and also transport it from one end to the other end resulting in a joint formation (Yu-hua et al., 2012). FSW technique can join both similar and dissimilar alloys including aluminum alloys. This technique has also shown a good capability to weld soft to hard materials like steel and aluminum. However, certain precautions need to be considered when the dissimilar materials and dissimilar alloys are welded. This includes material positioning during welding (advancing and retreating) as this plays a major role in the heat input which has a direct influence on the joint quality (Guo et al., 2014; Daniolos and Pantelis, 2017).

In as much as FSW can successfully be utilized in joining similar and dissimilar but there has not been a concrete conclusion regarding the optimized parameters to be used in welding certain materials. This is seen through the recent studies that are being conducted towards the optimization of the welding parameters. It is an undisputed fact that the welding parameters vary with the materials being welded hence the continuous optimization of the techniques. Peng et al. (2018) have investigated the welding parameters influence on the properties of dissimilar aluminum alloy joint with the focus on rotational speed. The two dissimilar aluminum alloys plates were used in conducting the study i.e. AA6061-T651 and AA5A06-H112. The one set of rotational speed was used in combination with two traverse speeds. There was a linear relationship observed between the rotational speed and the heat input which played a major role in the properties of the joint. The increase in rotational speed was led to an increase in heat input which also played a significant role in the stir zone grain size. This increase in heat input, however, led to an increase in grain size of the heat-affected zone (HAZ) which resulted in the drop in mechanical properties. This phenomenon encouraged the fracture to occur in the HAZ region.

Similar observations were also reported by various works (Dewangan et al., 2020; Kumar et al., 2020; Orłowska et al., 2020; Sameer and Birru, 2019; Uyyala and Pathri, 2020). The tool rotational and traverse speed play a more significant role in the heat input hence most works have focused on optimizing this parameter. Shunmugasundaram et al. (2020) have recently performed the welding parameters optimization on the joint form using AA6063 and AA5053 dissimilar plates. The statistical method called the Taguchi method was used to establish the proper parameter combination. The observation established from this work was that the traverse speed plays a major role in the enhancement of the tensile properties of the joint. Other optimization studies were performed on various alloys and materials and their findings yield different results

* Corresponding author.
E-mail address: msomiv@gmail.com (V. Msomi).

https://doi.org/10.1016/j.aime.2020.100002
Received 17 August 2020; Received in revised form 15 September 2020; Accepted 15 September 2020

Table 1
Chemical compositions for AA1050-H14 and AA6082-T6 (Mabuwa and Msomi, 2020; Alishavandi et al., 2020).

	Mg	Zn	V	Cr	Si	Mn	Fe	Cu	CuþAg	Al
AA1050-H14	0.05	0.05	0.05	–	0.05	0.05	0.4	0.05	–	Bal
AA6082-T6	1.1	0.20	–	0.25	0.90	0.70	0.50	–	0.10	Bal

Table 2
Nominal chemical composition of the HSS tool used (Bayer and Bacherer, 1989; Boccalini and Goldenstein, 2001).

Element	Cr	V	C	Si	Mo	W	Co	Fe
	4.13	1.98	0.83	0.33	5.00	6.13	–	Bal

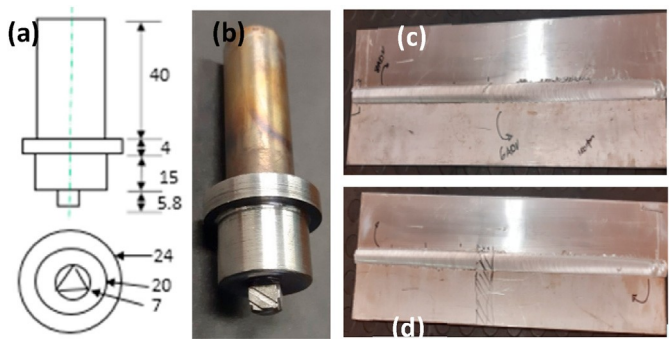

Fig. 1. (a) FSW tool, (b) Tool insert and (c) FSWed Plate and (d) FSPed- FSWed plate.

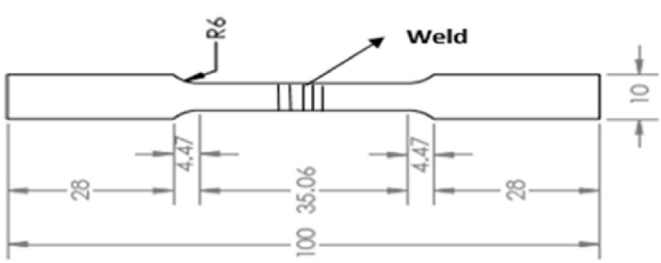

Fig. 2. Tensile specimen (dimensions in mm).

(Elnabi et al., 2019; Kumar et al., 2019; Kumar and Ramana, 2020; Li et al., 2019; Rzaev et al., 2019; Shaik et al., 2019; Suryanarayanan and Sridhar, 2020; Yuvaraj et al., 2020; Zhang et al., 2020). The use of the FSW technique to produce joints from various materials yields adverse outcomes like intermetallic compounds, porosity, etc. The existence of these defects in the joint affects the mechanical properties of the joint (Dong et al., 2019; Du et al., 2018; Jayaraj et al., 2017; Mahto et al., 2020; Muhammad et al., 2019; Wang et al., 2019). However, these defects can be alleviated through the application of post-processing techniques like friction stir processing (FSP). FSP is an advanced microstructural modification technique derived from FSW invented by The Welding Institute (Darras et al., 2007). FSP uses the same principle used by FSW but the only difference is that FSP does not join materials instead it modifies its microstructure (Mabuwa and Msomi, 2020; Seifiyan et al., 2019]. Its first discovery was associated with a single plate application but lately, it has been applied to the welded joints (Dinaharan et al., 2020; Kumar et al., 2020; Ma et al., 2020; Mabuwa and Msomi, 2020; Seifiyan et al., 2019). Recent developments have revealed that the FSP technique could be used in the formation of composite surfaces (Alishavandi et al., 2020; Balakrishnan et al., 2020; Deore et al., 2019; Gangil et al., 2019; Karpasand et al., 2020; Mazaheri et al., 2020; Sharma et al., 2019; Siddhardh et al., 2020).

The progress made on the FSP technology is still focusing on the single plate surfaces than joints. This then makes it difficult to understand the impact of employing FSP on the joints formed from dissimilar materials and alloys. Technology advances on a daily basis and new products are produced from various materials. This involves the use of similar and dissimilar materials in producing new better products. This then suggests that there will be a need to understand the performance of the joint formed from a similar and dissimilar material.

This paper reports on the influence of FSP on the microstructural arrangement of the joint formed from two distinct plates i.e. AA1050-H14 and AA6082-T6. Moreover, the influence of materials positioning on the microstructure being the major focus of this investigation.

2. Material and methodology

The materials used for the study were the commercially available aluminum alloys 1050-H14 and 6082-T6 plates with a thickness of 6 mm. The plates were cut into dimensions of 450 mm (length) by 70 mm (width) to fit on the fixture. The chemical compositions of the aluminum alloys are shown in Table 1. The friction stir welding technique was employed to join the two dissimilar materials. The LAGUN FA. 1-LA semi-automated milling machine was used to perform friction stir welding and friction stir processing. The high-speed tool steel used for FSW and FSP had a 5.8 mm pin length with a 7 mm in diameter. The shoulder diameter of the tool was 20 mm. The nominal chemical composition of the high-speed steel (HSS) tool is shown in Table 2. Fig. 1(a) shows the drawing of the tool used with dimensions in mm and Fig. 1(b) shows the image of the tool.

The performance of FSW and FSP was based on the rotational speed of 1200 rpm, welding speed of 40 mm/min, a spindle tool tilt of 2°, and these parameters were predetermined on the trial experiments (Gandra et al., 2011; Mishra and Ma, 2005; Sharma et al., 2015). The material positioning was varied during the FSW and FSP process i.e. the AA1050-H14 was placed interchangeably on the advancing side with AA6082-T6. The friction stir welded (FSWed) plate in Fig. 1(c) was later friction stir processed (FSPed) using the same parameters used for FSW (Gandra et al., 2011; Mishra and Ma, 2005; Sharma et al., 2015). Fig. 1(d) shows the friction stir processed FSWed plate.

The FSWed and FSPed welded joints were prepared for the metallographic examination and cut perpendicular to the welding direction, mounted, mechanically ground, polished, and etched using the Keller's reagent (1.5 ml HCl, 10 ml HNO_3, 1.0 ml HF, 87.5 ml distilled water, 10–60s immersing time) and Weck's reagent (1 g NaOH, 4 g $KMnO_4$, 100 ml distilled water, 15–20s immersing time). The Vicker's microhardness measurements were conducted on the middle cross-sections of the welded joints using a load of 2 kgf. The interval between the two points was 1.5 mm. The ASTM: E384-11 standard was used in performing microhardness testing. The tensile specimens were cut perpendicular to the welding direction into a dog bone shape according to ASTM E8M-04. The dimensions of the tensile specimen are shown in Fig. 2. The tensile tests were carried out at a head cross speed of 1 mm/min using a universal testing machine. The tensile data were logged using the Horizon software. The fracture surfaces of the tensile samples were observed using a scanning electron microscope (SEM).

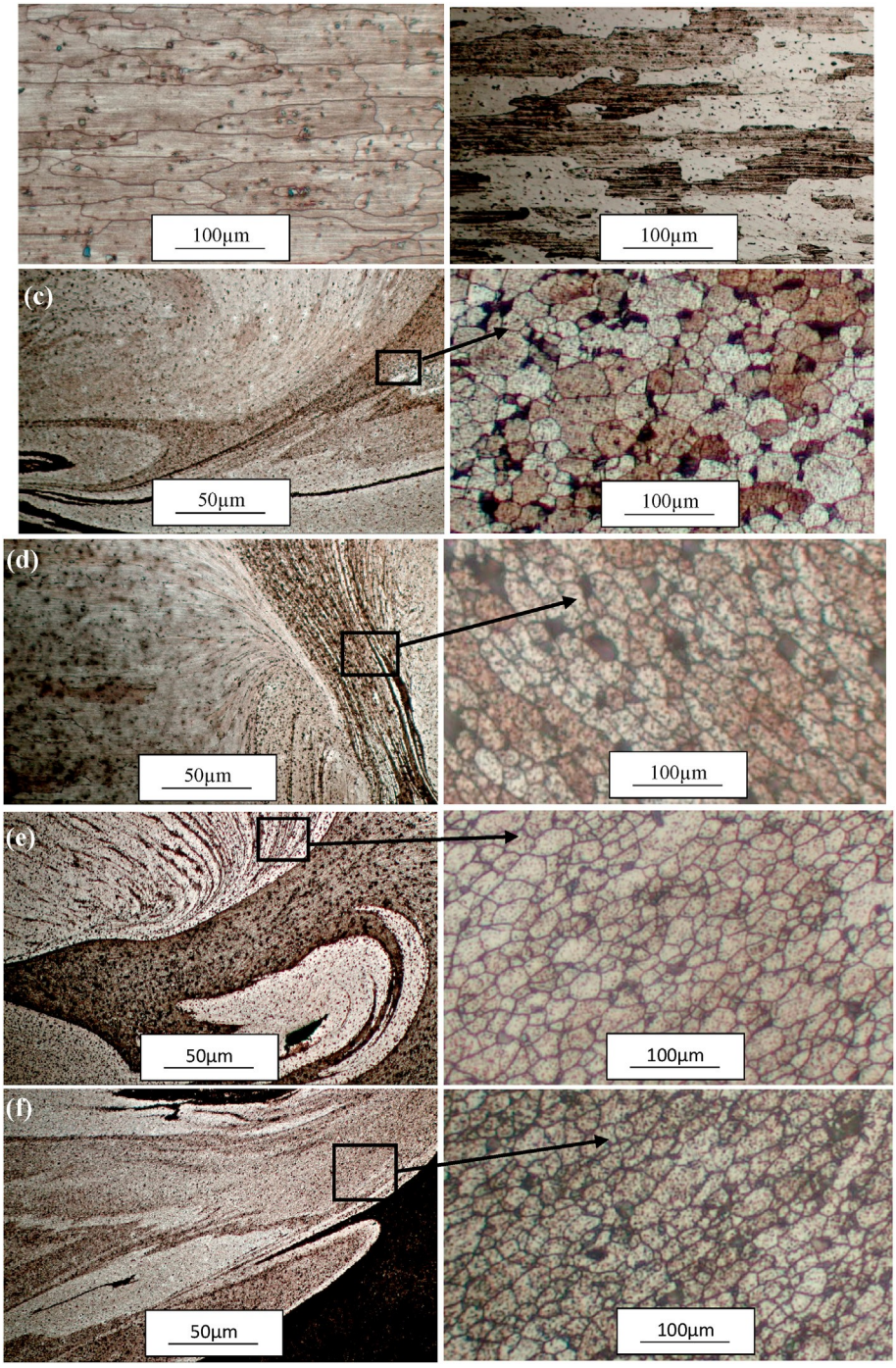

Fig. 3. Microstructural arrangement of (a) AA6082-T6 BM, (b) AA1050-H14 BM, (c) FSW AA1050 on the advancing side; (d) FSW AA6082 on the advancing side; (e) FSP AA1050 on the advancing side; (f) FSP AA6082 on the advancing side.

3. Results and discussions

3.1. Microstructural analysis

The microstructure of the friction stir welded (FSWed) dissimilar joint was studied in comparison to the friction stir processed (FSPed) dissimilar joint. This was performed to establish the significance of employing FSP on the FSWed dissimilar joint. The linear intercept method through ImageJ software was used in measuring the grain size. Fig. 3 shows the microstructure of the stir zone for the FSWed dissimilar joint and friction stir processed dissimilar joints. The microstructure of the base material AA6082-T6 shows the elongated morphology with a grain size average of 65.1 µm (see Fig. 3(a)). Fig. 3(b) presents the elongated grain structure for AA1050-H14 with an average size of 57.03 µm. The grain arrangement for the stir zone with AA1050 on the advancing side of the FSWed joint is shown in Fig. 3(c) while Fig. 3(d) depicts the stir zone grain arrangement when AA6082 was placed on the advancing side of the FSWed joint. The stir zone grain arrangement when AA1050 was placed on the advancing side during FSP is shown in Fig. 3(e) while Fig. 3(f) shows the stir zone morphology when AA6082 was placed on the advancing side during FSP.

The mean grain size of 33.18 µm was found when AA1050 was placed on the advancing side during FSW while the mean grain size of 28.11 µm was achieved when AA6082 was placed on the advancing side during

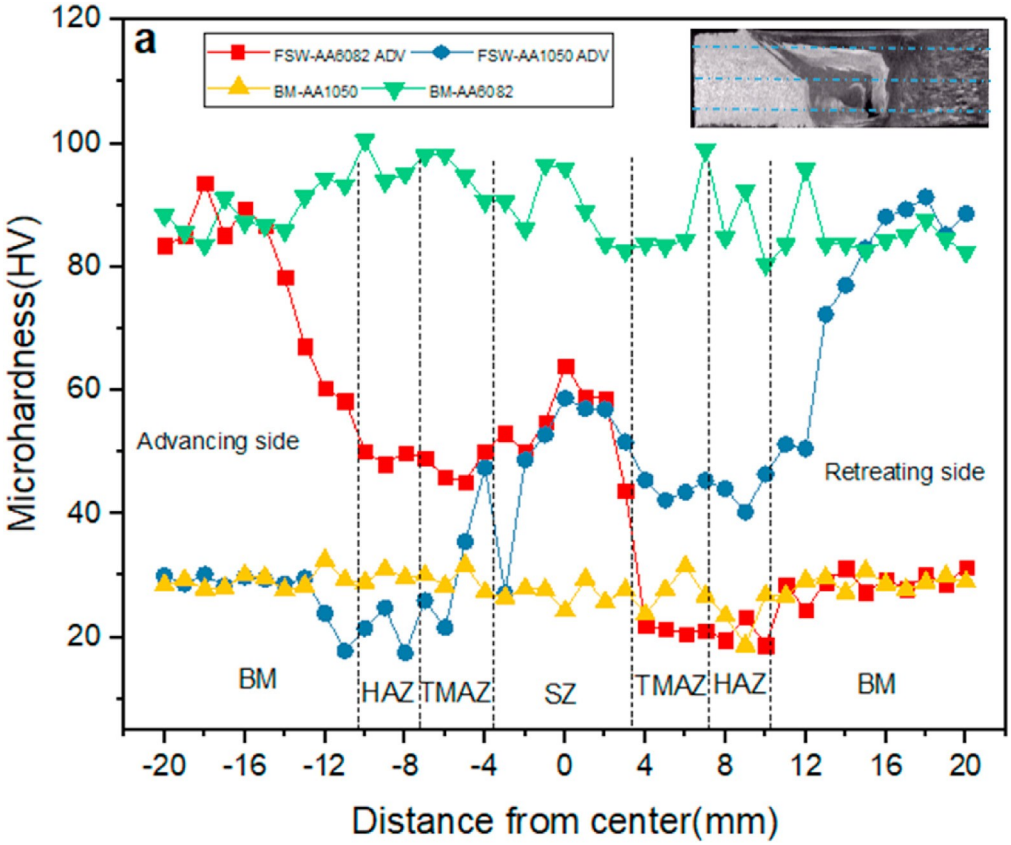

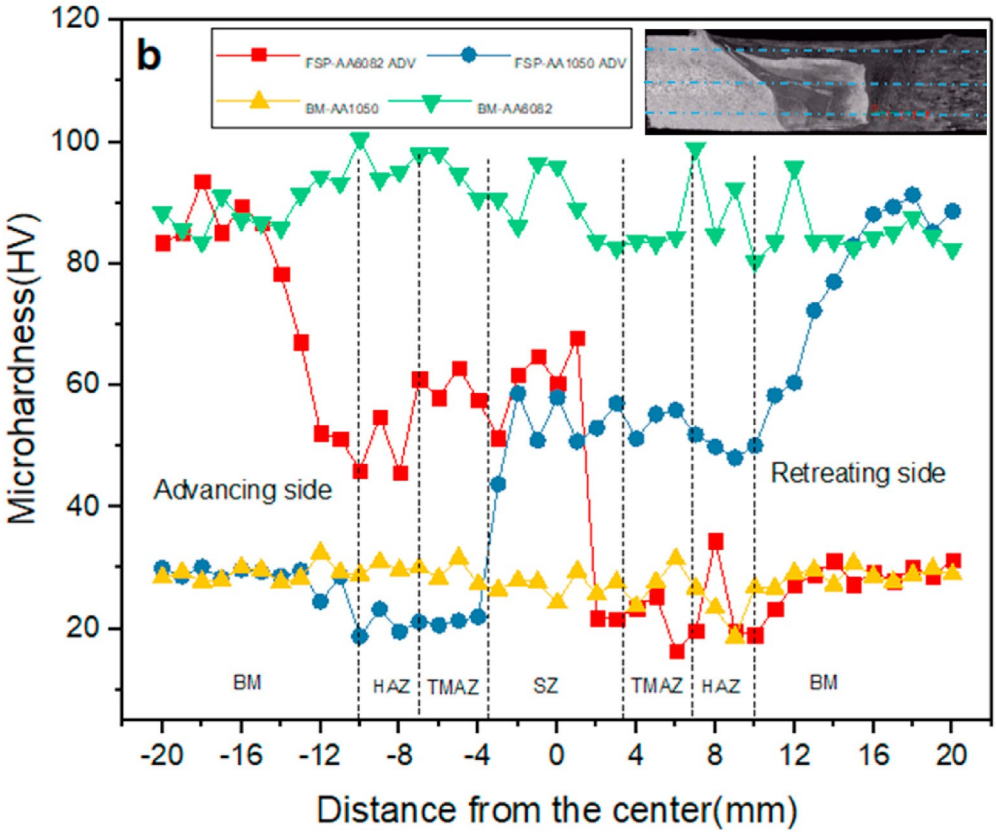

Fig. 4. Microhardness profile for (a) friction stir welded joint, (b) friction stir processed joint.

Table 3
Tensile properties of base materials, FSWed, and FSPed joints.

Joint/Material type	UTS (MPa)	YS (MPa)	Percentage elongation (%)
AA1050	105	85	6
AA6082	280	236	10
FSW- AA1050 ADV	46.1	28	20.5
FSW- AA6082 ADV	48	29	20.1
FSP-AA1050 ADV	81.5	58.6	22.1
FSP-AA6082 ADV	83.2	61.1	20.6

FSW. The mean grain size of 26.06 μm was achieved when the FSP was performed with AA1050 fixed on the advancing side. The lowest mean grain size of 21.37 μm was achieved when AA6082 was positioned on the advancing side during the FSP of the dissimilar joint. The grains of the friction stir processed stir zone were finer compared to the unprocessed ones due to the dynamic re-recrystallization experienced during FSP (Mabuwa and Msomi, 2020; Sathiskumar et al., 2013). It is good to note that the grain size phenomenon plays a significant role in the mechanical response of the joint (see tensile behavior analysis in Fig. 4). The vortex structures composed of alternative lamellae of AA1050 and AA6082 are observed in the stir zone. These vortex structures are the extruded material caused by the stirring action from the threaded tool. The presence of the extruded material in the stir zone suggests that different zones are occupied with different grains from the two base materials. Moreover, the grain size is also different from the advancing side, retreating side, the top, and the root of the joint. This phenomenon is normal when the joint is produced from materials with distinct properties using the threaded tool (Cavaliere et al., 2009). Moreover, the phenomenon of grain size is mostly depending on the temperature gradients and the strain rate and these two are conditions are influenced by the positioning of the materials (Lee et al., 2003).

3.2. Microhardness analysis

The FSWed dissimilar joint was also studied comparatively to the FSPed dissimilar joint. Fig. 4(a) shows the microhardness of FSWed dissimilar joint formed using AA1050 and AA6082 plates whereas Fig. 4(b) presents the microhardness profile for the FSPed dissimilar joint. The microhardness was measured on the regions indicated on the inserted picture of each microhardness profile. The microhardness at the HAZ and TMAZ regions is lower than that of the stir zone on both FSWed and FSPed joints. The drop in microhardness is caused by the coarsening due to the high-temperature gradient, the disappearance of GP zones, and the formation of overaged precipitates at the HAZ and TMAZ regions, respectively. The increase in microhardness at the stir zone is observed in both FSWed and FSPed dissimilar joints. This microhardness increase is attributed to the greater dissolution which is accompanied by the formation of the new strengthening precipitates (Cavaliere et al., 2009; Cabibbo et al., 2007). The microhardness at the TMAZ region for the advancing side is lower compared to that for the retreating side when AA1050 is placed on the advancing side for both FSWed and FSPed joints. The difference in microhardness in this region is due to highly elongated grains with fine cells of AA6082 dominating the retreating side than the advancing side (Cabibbo et al., 2007). The microhardness at the TMAZ region of the advancing side is higher compared to that for the retreating side when AA6082 is on the advancing side for both FSWed and FSPed joints. This then suggests that there was a phenomenon shift observed when the same material was on the retreating side. It is also observed that the microhardness at the stir zone for the FSPed joint is higher compared to that of the FSWed joint. This is due to the dynamic recrystallization occurred during the FSP process (Yu-hua et al., 2012; Kumar and Ramana, 2020; Li et al., 2019; Mahto et al., 2020; Rzaev et al., 2019; Shaik et al., 2019; Yuvaraj et al., 2020; Zhang et al., 2020). In both FSWed and FSPed, it was observed that the best microhardness results were produced when AA1050 was placed on the advancing than on the retreating side. The improved microhardness at the stir zone indicates proper material mixing (Cavaliere et al., 2009).

3.3. Tensile properties

Table 3 shows the tensile properties of the base materials, FSWed, and FSPed joints. The graphical representation of these values is shown in Fig. 5. The symbols A and B represent the FSWed dissimilar joint whereas A2 and B2 represent the FSPed dissimilar joint. Symbol A represents the FSW dissimilar joint produced when AA6082 was placed on the advancing side while B represents the FSWed dissimilar joint produced when AA1050 was positioned on the advancing side. Symbol A2 represents the FSPed dissimilar joint produced with AA6082 on the advancing side whereas B2 represents FSPed dissimilar joint with AA1050 on the advancing side. It was observed that the FSWed dissimilar joint produced

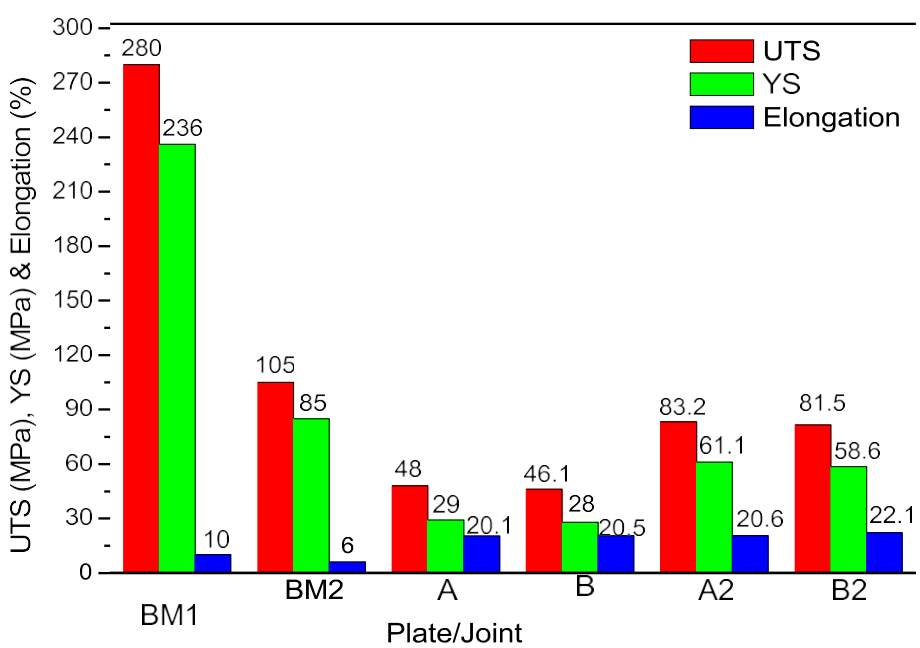

Fig. 5. Tensile properties.

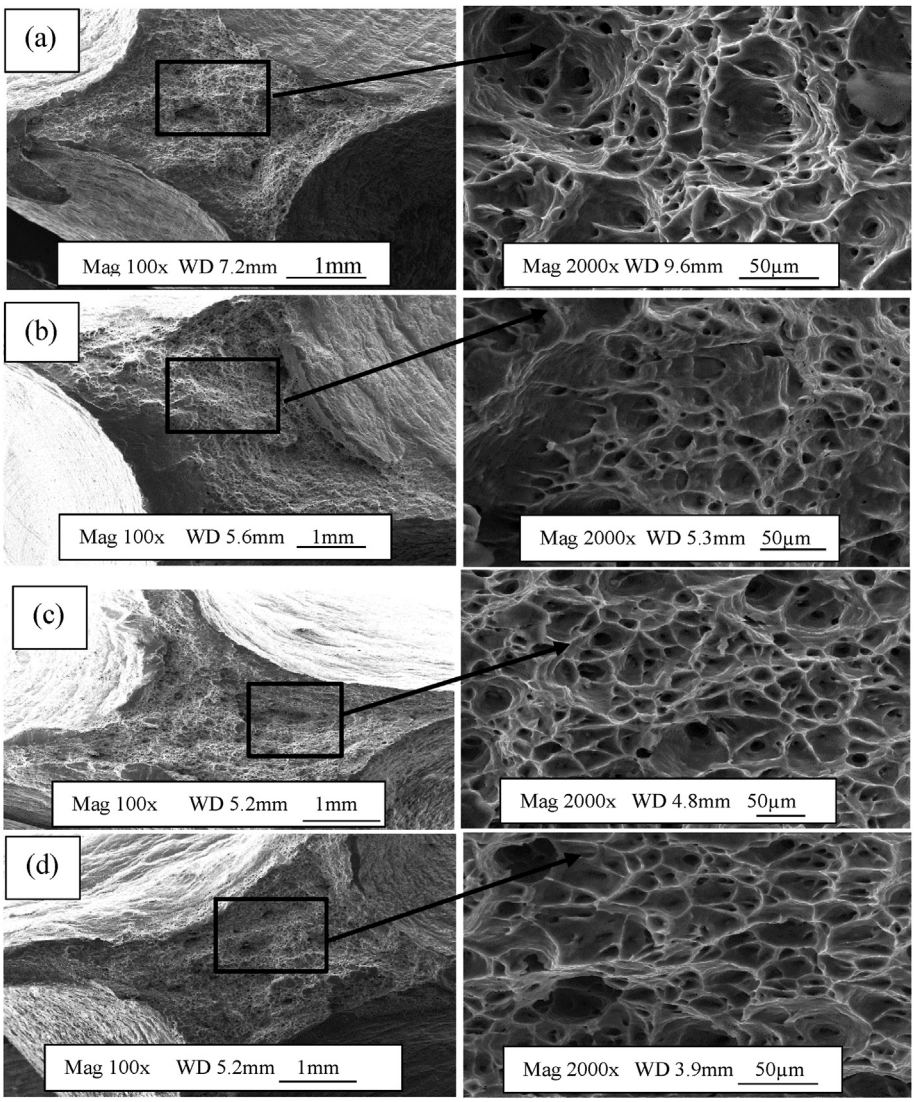

Fig. 6. Fractographs of tensile test specimens, (a) FSW AA1050 on the advancing side; (b) FSW AA6082 on the advancing side; (c) FSP AA1050 on the advancing side; (d) FSP AA6082 on the advancing side.

higher ultimate tensile strength (UTS) and yield strength (YS) when AA6082 was on the advancing side than when AA1050 on the advancing side and similar behavior was also observed on the FSPed dissimilar joint. The UTS and YS for the FSPed joint were found to be higher compared to that of the FSWed dissimilar joint. However, UTS and YS for both joints were lower compared to the UTS and YS for both base materials (BM). The percentage elongation for both FSWed and FSPed dissimilar joints were found to be higher than both base materials. This phenomenon is suggested to be caused by the microstructural arrangement that was influenced mostly by material positioning (Guo et al., 2014; Lee et al., 2003; Mabuwa and Msomi, 2020; Sathiskumar et al., 2013).

3.4. Fractured surface morphology

The tensile test fractured surfaces were further examined at low and high magnification to understand fracture mechanism. Fig. 6 shows the fractographs for the FSWed and FSPed dissimilar joints. Fig. 6(a) and (b) show the fractography for the FSWed joint when AA1050 on the advancing side and AA6082 on the advancing side respectively. The fractured surface of the FSPed joint with AA1050 on the advancing side is shown in Fig. 6(c) and the FSPed joint with AA6082 on the advancing side is shown in Fig. 6(d). All the surfaces show dimples of various sizes and depths. The presence of dimples is the indication of ductile failure mode (Orłowska et al., 2020; Elnabi et al., 2019; Kumar et al., 2019; Kumar and Ramana, 2020; Shunmugasundaram et al., 2020; Suryanarayanan and Sridhar, 2020; Dong et al., 2019; Darras et al., 2007). The FSPed surfaces are dominated by the finer dimples compared to those of the FSWed surfaces. This phenomenon is caused by the grain refinement which contributes to the inhibition of dislocation movement (delayed micro-voids formation) hence an improved ductility on the FSPed joints (Paidar et al., 2020; Sameer and Birru, 2019).

4. Conclusions

The microstructural evaluation of the FSWed and FSPed dissimilar joints was carried out successfully. The following conclusions were made based on the results:

- The joint formed from dissimilar material gets dominated by the material with higher strength. This behavior was observed on both FSWed and FSPed joints.
- The positioning of AA6082 material on the advancing side contributed to the refinement of grains at the stir zone.

- The microhardness at the stir zone is higher when AA6082 is positioned on the advancing side for both FSWed and FSPed joints.
- The positioning of AA1050 on the advancing side contributed to the enhancement of the percentage elongation while AA6082 contributed to the enhancement of the tensile and yield strength.

In summary, the results reveal that the positioning of any material on the advancing side during the performance of FSW and FSP influences the joint properties.

Data availability

The data used to produce this paper can be obtained from the corresponding author upon request.

Funding statement

The would like to thank funding received from the National Research Foundation through Thuthuka Grant [118046].

Conflicts of interest

The authors declare that no conflict of interest may arise from this work.

References

Boccalini, M., Goldenstein, H., 2001. Solidification of high speed steel. Int. Mater. Rev. 46 (2), 92–107.
Cabibbo, M., McQueen, H.J., Evangelista, E., Spigarelli, S., Di Paola, M., Falchero, A., 2007. Microstructure and mechanical property studies of AA6056 friction stir welded plate. Mater. Sci. Eng. 460 (461), 86–94.
Cavaliere, P., De Santis, A., Panella, F., Squillace, A., 2009. Effect of welding parameters on mechanical and microstructural properties of dissimilar AA6082–AA2024 joints produced by friction stir welding. Mater. Des. 30 (3), 609–616.
Daniolos, N.M., Pantelis, D.I., 2017. Microstructural and mechanical properties of dissimilar friction stir welds between AA6082-T6 and AA7075-T651. Int. J. Adv. Manuf. Technol. 88, 2497–2505.
Darras, B.M., Omar, M.A., Khraisheh, M.K., 2007. Experimental thermal analysis of friction stir processing. THERMEC 539–543, 3801–3806.
Gandra, J., Miranda, R., Vilaca, P., Velhinho, A., Teixeira, J.P., 2011. Functionally graded materials produced by friction stir processing. J. Mater. Process. Technol. 211, 1659–1668.
Gangil, N., Maheshwari, S., Siddiquee, A.N., Abidi, M.H., El-Meligy, M.A., Mohammed, J.A., 2019. Investigation on friction stir welding of hybrid composites fabricated on Al–Zn–Mg–Cu alloy through friction stir processing. Journal of Materials Research and Technology 8 (5), 3733–3740.
Karpasand, F., Abbasi, A., Ardestani, M., 2020. Effect of amount of TiB2 and B4C particles on tribological behavior of Al7075/B4C/TiB2 mono and hybrid surface composites produced by friction stir processing. Surf. Coating. Technol. 390, 125680.
Kumar, K.S., Devaraju, A., Manichandra, B., 2020. Investigating the mechanical and metallographic properties of FSWed dissimilar 6061 & 2024 aluminum alloys by varying distinctive parameters. Mater. Today: Proceedings 24 (2), 880–886.
Paidar, M., Vignesh, R.V., Khorram, A., Ojo, O.O., Rasoulpouraghdam, A., Pustokhina, I., 2020. Dissimilar modified friction stir clinching of AA2024-AA6061 aluminum alloys: effects of materials positioning. Journal of Materials Research and Technology 9 (3), 6037–6047.
Peng, G., Ma, Y., Hu, J., Jiang, W., Huan, Y., Chen, Z., Zhang, T., 2018. Nanoindentation hardness distribution and strain field and fracture evolution in dissimilar friction stir-welded AA 6061-AA 5A06 aluminum alloy joints. Advances in Materials Science and Engineering 1–11. https://doi.org/10.1155/2018/4873571, 4873571.
Wang, T., Sidhar, H., Mishra, R.S., Hovanski, Y., Upadhyay, P., Carlson, B., 2019. Evaluation of intermetallic compound layer at aluminum/steel interface joined by friction stir scribe technology. Mater. Des. 174, 107795.
Yu-hua, C., Quan, N.I., Li-ming, K.E., 2012. Interface characteristic of friction stir welding lap joints of Ti/Al dissimilar alloys. Trans. Nonferrous Metals Soc. China 22 (2), 299–304, 2012.
Yuvaraj, K.P., Varthanan, P.A., Haribabu, L., Madhubalan, R., Boopathiraja, K.P., 2020. Optimization of FSW tool parameters for joining dissimilar AA7075-T651 and AA6061 aluminum alloys using Taguchi Technique. Mater. Today: Proceedings, https://doi.org/10.1016/j.matpr.2020.02.942. In press.
Mabuwa, S., Msomi, V., 2020. The effect of friction stir processing on the friction stir welded AA1050-H14 and AA6082-T6 joints. Mater. Today: Proceedings 26 (2), 193–199.
Mazaheri, Y., Jalilvand, M.M., Heidarpour, A., Jahani, A.R., 2020. Tribological behavior of AZ31/ZrO2 surface nanocomposites developed by friction stir processing. Tribol. Int. 143, 106062.
Mishra, R.S., Ma, Z.Y., 2005. Friction stir welding and processing. Mater. Sci. Eng., R 50 (1–2), 1–78.
Siddhardh, K., Chandra, M.S., Surya, S., Kumaran, S.S., 2020. An investigation on friction welding of tube to tube plate by using friction stir processing with CNT and Si3N4 composites. Mater. Today: Proceedings 22 (4), 2452–2459.
Suryanarayanan, R., Sridhar, V.G., 2020. Experimental investigation on the influence of process parameters in Friction stir spot welded dissimilar aluminum alloys. Mater. Today: Proceedings 27 (1), 529–533.
Uyyala, S.B., Pathri, S., 2020. Investigation of tensile strength on friction stir welded joints of dissimilar aluminum alloys. Mater. Today: Proceedings 23 (3), 469–473.
Dinaharan, I., Zhang, S., Chen, G., Shi, Q., 2020. Development of titanium particulate reinforced AZ31 magnesium matrix composites via friction stir processing. J. Alloys Compd. 820, 15307.
Dong, Z., Song, Q., Ai, X., Lv, Z., 2019. Effect of joining time on intermetallic compound thickness and mechanical properties of refill friction stir spot welded dissimilar Al/Mg alloys. J. Manuf. Process. 42, 106–112.
Ma, C.Y., Zhou, L., Zhang, R.X., Li, D.G., Shu, F.Y., Song, X.G., Zhao, Y.Q., 2020. Enhancement in mechanical properties and corrosion resistance of 2507 duplex stainless steel via friction stir processing. Journal of Materials Research and Technology 9 (4), 8296–8305.
Kumar, S.R., KajaBanthaNavas, R., Sujeeth, P.S., 2019. Multiple response optimization studies for dissimilar friction stir welding parameters of 6061 to 7075 aluminum alloys. Mater. Today: Proceedings 16 (2), 405–412.
Lee, W., Yeon, Y., Jung, S., 2003. The joint properties of dissimilar formed Al alloys by friction stir welding according to the fixed location of materials. Scripta Mater. 49 (5), 423–428.
Li, G., Zhou, L., Zhou, W., Song, X., Huang, Y., 2019. Influence of dwell time on microstructure evolution and mechanical properties of dissimilar friction stir spot welded aluminum–copper metals. Journal of Materials Research and Technology 8 (3), 2613–2624.
Dewangan, S.K., Tripathi, M.K., Manoj, M.K., 2020. Effect of welding speeds on microstructure and mechanical properties of dissimilar friction stir welding of AA7075 and AA5083 alloy. Mater. Today: Proceedings 27 (3), 2713–2717.
Sharma, V., Prakash, U., Kumar, B.V.M., 2015. Surface composites by friction stir processing: a review. J. Mater. Process. Technol. 224, 117–134.
Sharma, R., Singh, A.K., Arora, A., Pati, S., De, P.S., 2019. Effect of friction stir processing on corrosion of Al-TiB2 based composite in 3.5 wt.% sodium chloride solution. Trans. Nonferrous Metals Soc. China 29 (7), 1383–1392.
Shunmugasundaram, M., Kumar, A.P., Sankar, L.P., Sivasankar, S., 2020. Optimization of process parameters of friction stir welded dissimilar AA6063 and AA5052 aluminum alloys by Taguchi technique. Mater. Today: Proceedings 27 (2), 871–876.
Guo, J.F., Chen, H.C., Sun, C.N., Bi, G., Sun, Z., Wei, J., 2014. Friction stir welding of dissimilar materials between AA6061 and AA7075 Al alloys effects of process parameters. Mater. Des. 56, 185–192.
Jayaraj, R.K., Malarvizhi, S., Balasubramanian, V., 2017. Optimizing the micro-arc oxidation (MAO) parameters to attain coatings with minimum porosity and maximum hardness on the friction stir welded AA6061 aluminum alloy welds. Defence Technology 13 (2), 111–117.
Mahto, R.P., Kumar, R., Pal, S.K., 2020. Characterizations of weld defects, intermetallic compounds and mechanical properties of friction stir lap welded dissimilar alloys. Mater. Char. 160, 110115.
Dawes, C.J, Thomas, W.M., 1996. Friction stir process welds aluminum alloys. Weld. J. 75, 41–45.
Deore, H.A., Mishra, J., Rao, A.G., Mehtani, H., Hiwarkar, V.D., 2019. Effect of filler material and post process ageing treatment on microstructure, mechanical properties and wear behaviour of friction stir processed AA7075 surface composites. Surf. Coating. Technol. 374, 52–64.
Du, Z., Chen, H., Tan, M.J., Bi, G., Chua, C.K., 2018. Investigation of porosity reduction, microstructure and mechanical properties for joining of selective laser melting fabricated aluminum composite via friction stir welding. J. Manuf. Process. 36, 33–43.
Elnabi, M.M.A., Elshalakany, A.B., Abdel-Mottaleb, M.M., Osman, T.A., Mokadem, A.E., 2019. Influence of friction stir welding parameters on metallurgical and mechanical properties of dissimilar AA5454–AA7075 aluminum alloys. Journal of Materials Research and Technology 8 (2), 1684–1693.
Sameer, M.D., Birru, A.K., 2019. Mechanical and metallurgical properties of friction stir welded dissimilar joints of AZ91 magnesium alloy and AA 6082-T6 aluminium alloy. Journal of Magnesium and Alloys 7 (2), 264–271.
Sathiskumar, R., Murugana, N., Dinaharan, I., Vijay, S.J., 2013. Characterization of boron carbide particulate reinforced in situ copper surface composites synthesized using friction stir processing. Mater. Char. 84, 16–20.
Seifiyan, H., Sohi, M.H., Ansari, M., Ahmadkhaniha, D., Saremi, M., 2019. Influence of friction stir processing conditions on corrosion behavior of AZ31B magnesium alloy. Journal of Magnesium and Alloys 7 (4), 605–616.
Shaik, B., Gowd, G.H., Prasad, B.D., 2019. Experimental and parametric studies with friction stir welding on aluminum alloys. Mater. Today: Proceedings 19 (2), 372–379.
Alishavandi, M., Khollari, M.A.R., Ebadi, M., Alishavandi, S., Kokabi, A.H., 2020. Corrosion-wear behavior of AA1050/mischmetal oxides surface nanocomposite fabricated by friction stir processing. J. Alloys Compd. 832, 153964.
Balakrishnan, M., Dinaharan, I., Kalaiselvan, K., Palanivel, R., 2020. Friction stir processing of Al3Ni intermetallic particulate reinforced cast aluminum matrix composites: microstructure and tensile properties. Journal of Materials Research and Technology 9 (3), 4356–4367.
Bayer, A.M., Bacherer, B.A., 1989. High speed tool steels. ASM Handbook 16, 51–59.

Kumar, H., Prasad, R., Kumar, P., Tewari, S.P., Singh, J.K., 2020. Mechanical and tribological characterization of industrial wastes reinforced aluminum alloy composites fabricated via friction stir processing. J. Alloys Compd. 831, 154832.
Kumar, H.M.A., Ramana, V.V., 2020. Influence of tool parameters on the tensile properties of friction stir welded aluminum 5083 and 6082 alloys. Mater. Today: Proceedings 27 (2), 951–957.
Muhammad, N.A., Wu, C.S., Tian, W., 2019. Effect of ultrasonic vibration on the intermetallic compound layer formation in Al/Cu friction stir weld joints. J. Alloys Compd. 785, 512–522.
Orłowska, M., Brynk, T., Hütter, A., Goliński, J., Enzinger, N., Olejnik, L., Lewandowska, M., 2020. Similar and dissimilar welds of ultrafine grained aluminum obtained by friction stir welding. Mater. Sci. Eng. 777, 139076.
Rzaev, R., Chularis, A., Smirnov, V., Semyenova, L., 2019. The influence of the friction stir welding parameters on the formation of welded joint of aluminum and copper alloys. Mater. Today: Proceedings 11 (1), 534–542.
Sameer, M.D., Birru, A.K., 2019. Mechanical and metallurgical properties of friction stir welded dissimilar joints of AZ91 magnesium alloy and AA 6082-T6 aluminum alloy. Journal of Magnesium and Alloys 7 (2), 264–271.
Zhang, C., Cao, Y., Huang, G., Zeng, Q., Zhu, Y., Huang, X., Li, N., Liu, Q., 2020. Influence of tool rotational speed on local microstructure, mechanical and corrosion behavior of dissimilar AA2024/7075 joints fabricated by friction stir welding. J. Manuf. Process. 49, 214–226.

Questões

1. ***Estabeleça os elementos encontrados na Conclusão do estudo em tela.***

2. ***Explicite as discussões da tabela 3, descrevendo-a conforme o artigo.***

3. ***Explique o material e metodologias usados neste estudo.***

4. ***Em que consiste a técnica FSW?***

5. ***Elabore um resumo (abstract) em língua portuguesa para o texto em tela em cerca de 80 palavras, indicando inclusive palavras-chave.***